Mechanical behavior of sandwich panels with curauá fiber reinforced composite skins and autoclaved aerated concrete core

Isabela de Paula Salgado[1], Flávio de Andrade Silva[2]

[1]*Institute of Construction Materials, Technische Universität Dresden*
Dresden, Germany
dpsalgado@unu.edu, isabela.de_paula_salgado@tu-dresden.de
[2]*Dept. of Civil and Environmental Engineering, Pontifícia Universidade Católica do Rio de Janeiro*
Rua Marques de São Vicente 225, 22453-900, Rio de Janeiro -RJ, Brazil
fsilva@puc-rio.br

Abstract. A curauá fiber-reinforced aerated concrete sandwich panel was developed as a sustainable, lightweight, and low-cost alternative construction material. Each composite skin consisted of long unidirectional aligned curauá fibers, applied by a cast hand layup technique, and a cementitious matrix with 50% of Portland cement replacement by pozzolanic materials. The mechanical properties of the sandwich panels and their components were investigated. The skins displayed a strain-hardening response and multiple cracking behavior. Strength, deformation capacity, and cracking mechanisms of the composite laminates are presented. The sandwich panels' monotonic and cyclic four-point bending responses were evaluated. The bonding between the composite layers and the autoclaved aerated concrete (AAC) core was assessed through pull-off tests and microscopic imaging. The results revealed the efficiency of the cementitious layers in providing a more ductile behavior and a higher flexural strength to the material. The ductility properties of the AAC core were improved when assisted by the skin layers in the sandwich structure. A deflection-softening behavior and a satisfactory post-peak ductility were observed in the cyclic bending tests. Failure mechanisms, strength, and toughness are reported.

Keywords: sandwich panels, autoclaved aerated concrete, cementitious composites, natural fibers, flexural strength.

1 Introduction

In recent years, there has been an increasing interest in sustainable materials, particularly renewable and biodegradable resources. Literature works indicate the potential of natural fibers to replace their synthetic counterparts, as they are generally light and thermally insulating, with high tensile strength and stiffness [1, 2]. Such is the case of natural fiber reinforced composites in comparison to glass and polypropylene fiber-reinforced alternatives, since the first provides comparable performance but with enhanced absorption capacity and reduced pollutant emissions [3, 4]. Natural reinforcement can improve the material's ductility and post-cracking toughness [5]. The performance efficiency depends on the fiber morphology, orientation, and quantity; fiber-matrix interface; stress transfer between matrix and reinforcement [6]. On that account, the matrix's strain capacity is lower than the fiber's, so it fails before the reinforcement's total capacity is reached. The fibers then intersect the cracks, contributing to the material's energy dissipation via pull-out and debonding [7].

Curauá (*Ananas erectifolius*) stands out among traditional Brazilian fibers due to its superior tensile strength compared to sisal, jute, and coir [5,6]. Curauá fibers are also cheaper than flax, polypropylene, and glass fibers [10]. Several studies present good results with Curauá reinforced composites, owing to their ductility and post-cracking strength [7,8] – as is the case of Strain-Hardening Cementitious Composites (SHCC), which are reportedly suitable for facades, repair, and structural uses [12,13].

Using a cementitious matrix with natural fibers as reinforcement, however, demands additional measures to protect the composite's integrity. The cement paste has a negative effect on the fibers, presumably leading to early loss of composite strength, as demonstrated by several research findings [9,10].Surface treatments on fibers can change their water absorption capacity and improve their compatibility with the matrix [15,16]. Partially replacing cement with pozzolanic materials has also proven effective in terms of durability [11,12] and sustainability issues related to CO2 emissions and other greenhouse gases [20, 21].

Additionally, to reduce gas emissions and the need for refrigeration systems, materials with thermal insulation are recommended. One of the options is autoclaved aerated concrete (AAC), whose production is energy efficient

and whose gas emissions (CO2, CO, NOx) are comparatively lower than standard industrial processes [22]. AAC is lightweight, isotropic, and recyclable [15,17,18]. The material's high porosity is responsible for its low specific weight and good thermal performance [14–16], but also compromises its compressive strength and, consequently, possible structural applications. The industry's need for new high-performance materials is met by sandwich structures. Sandwich panels are usually light, stiff, and easy to manufacture [28]. Sandwich panels with thin ductile layers and a thermal core allow for efficient structural, acoustic, and thermal building systems [29].

This study proposes a solution that combines sustainability and mechanical performance: sandwich panels with natural fiber-reinforced composite layers for ductility and resistance, and an AAC core for insulation. Panels and composites were tested in monotonic four-point bending. The sandwich panels were also subjected to cyclic bending tests to investigate the mechanisms of degradation and energy loss. We calculated flexural strength and toughness, and studied failure mechanisms. SEM, optical microscopy, and pull-off tests were used to evaluate the AAC-composite laminate bond.

2 Experimental program

2.1 Materials

The Curauá fibers used in this work come from the *Ananas comosus erectifolius* plant, whose leaves were obtained from a plant farm in Aurora do Pará, Brazil. To be employed as reinforcement, the fibers had to be cleaned for an hour in hot water (70-80^{o}C) followed by 48 hours of natural drying. The dry fiber bundles were meticulously brushed into filaments, which were then divided into 350 mm layers. Martel et al. [17] describe in detail the microstructure, water absorption capacity, and mechanical performance of the fibers employed in this technique. The curauá filaments have a tensile strength of 872 (326) MPa and a Young's modulus of 16.5 (5.7) GPa.

In addition to Lafarge-CPV-ARI Holcim's Brazilian Portland cement, Metacaulim do Brasil Indstria e Comércio Ltda's Metakaolin (MK) were used in the composite matrix. The components were blended 1:1:0.4 (binder: sand: water), with the binder (cementitious materials) being 50% Portland cement, 40% MK, and 10% fly ash. The use of pozzolanic elements in the mix design lowered the calcium hydroxide content, enhancing the fiber durability in the cementitious matrix. The appropriate workability of the matrix was achieved by adding 2.5 percent superplasticizer Plastol 4100 to the binder weight, which delivered 400 mm of slump flow according to ASTM C230/C230M [30]. The resultant matrix displayed 74 MPa of compressive strength.

2.2 Sandwich panels manufacturing

Sandwich panels of 350 x 60 x 90 mm (length x width x thickness) were produced, consisting of two fiber-reinforced composite layers of 10 mm each and a 70 mm thick precast autoclaved aerated concrete core. Lightweight AAC blocks were provided by Precon.

In a planetary mixer, the sand and cementitious ingredients were first combined with water for 1 min 30 s. After homogenization, the superplasticizer was applied gradually and mixed for 4 minutes. Before molding, the curauá fibers were brushed, split into bundles, trimmed to length, and then weighted. The bundles were then submerged for 2 hours to achieve saturation and avoid volumetric differences when placed in the matrix. After drying, each fiber layer was brushed again to ensure proper reinforcement alignment in the matrix.

Composites of 350 mm x 60 mm x 10 mm (length x width x thickness) were produced by hand casting long unidirectional curauá fibers (7.5% volume proportion). The three layers had the same approximate weight (4.2-5 g). The laminates wer then cast directly on the AAC blocks, which had been moistened to avoid water absorption during the initial mortar layer. The outer layers were cast individually, taking two days to be produced. The panels were then demolded and cured for 28 days in a humid chamber. No interlayer connectors were employed, the composite-core adhesion was dependent on the cement and AAC's porous surface..

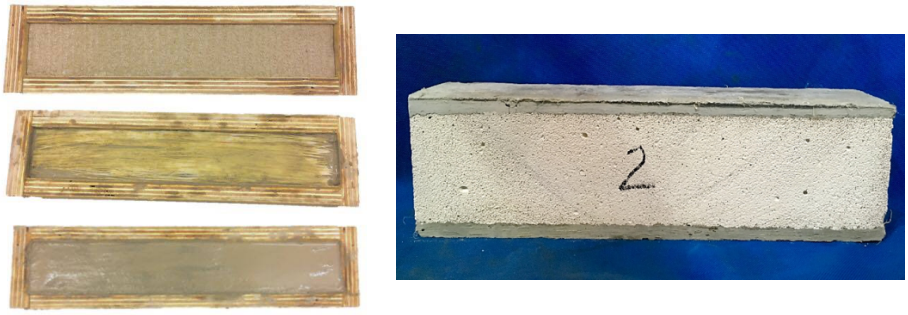

(a) (b)

Figure 1: Sandwich panels : (a) production steps; (b) final product.

2.3 Testing

2.3.1 Monotonic four-point bending tests

The overall performance of sandwich panels and its components (layers and core) was assed by four-point bending tests. Three sandwich panels were tested on a MTS 204.63 with a 270 mm span and a 90 mm gap between the load points. Two displacement transducers at mid-span detected the specimens' vertical displacement. The bending tests were performed with a 1 mm/min displacement control. Figure 2a shows the test setup.

Eight composites were tested for flexural performance in accordance with ASTM C1341 [23]. The laminates were tested on a 500 kN MTS 810. The system had a 2.5 kN load cell. Two transducers on the composite's upper surface detected the specimens' vertical displacement. The test was performed at a displacement rate of 1mm/min over a 270 mm span.

2.3.2 Cyclic four-point bending tests

The cyclic bending tests used the identical three sandwich panels (350 mm x 60 mm x 90 mm) as the monotonic testing. Ten cycles of LVDT displacement control were used to produce fixed points of deflection: 0.2, 0.4, and 0.8 mm at 0.1 mm/min; 1.0, 2.0, 3.0, 4.0, and 5.0 mm at 0.5 mm/min; and lastly 7.5 and 10.0 mm at 1 mm/min. In load control mode, the specimen is unloaded at a rate of 1 kN/min until a minimal force level is attained. Sensitivity was increased by using two LVDTs in the middle of the specimens' span: one 5 mm high and one 50 mm low. The 5 mm LVDT recorded the cyclic deflection with 3 mm precision. The control was subsequently given to the 50 mm LVDT, which completed the remaining cycles. The LVDTs magnetic base was grounded, and the 50 mm LVDT was inverted to reduce spring pressure and noise. Figure 2-b shows the setup.

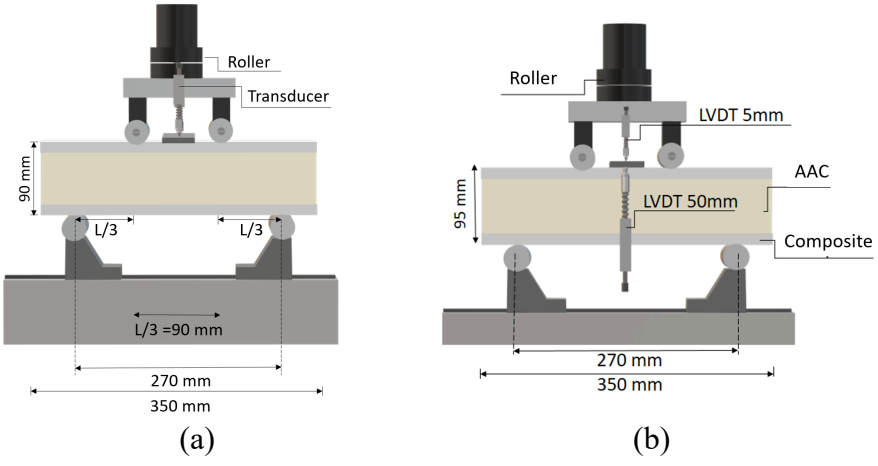

(a) (b)

Figure 2: Sheme for the four-point bending tests on sandwich panels: (a) monotonic; (b) cyclic.

2.4 Results and discussion

The three tested sandwich panels showed satisfactory deflection capacity., despite the steady loss of load capacity, Figure 3 compares the tested panels' load-deflection behavior to AAC blocks. Until the first fractures develop, the core and skin layers behave linear-elasticaly. Then, many cracks in the core layer generate a dramatic decline in force. Reduced adhesion between parts, crack propagation, and stress prolonging cause significant loss in stiffness and strength. The sandwich structure improves flexural strength and energy absorption capacity over plain AAC blocks.

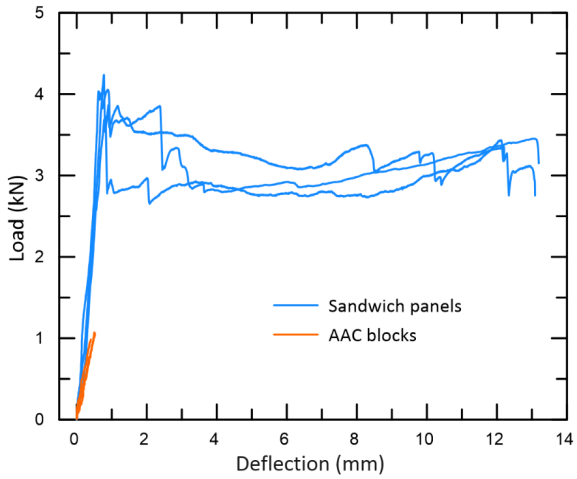

Figure 3: Load-deflection curves of all tested specimens of sandwich panels and AAC blocks subjected to monotonic four-point bending tests

The sample' apparent flexural strength was determined using standard bending formulae. The test specimens' flexural characteristics and load-carrying capacity are comparable to sandwich panels of similar structure, such as Dey et al.'s [35], with a 2.4 Mpa flexural strength and 1.34 mm deflection for sandwich panels with a AAC core and two layers of alkali-resistant glass (ARG) textiles. The developed curauá fiber reinforced composites (CFRC-AAC) panels had a similar apparent flexural strength (2.2 MPa) to the ARGFRC-AAC panels (2.4 MPa). The long curauá fiber-reinforced laminates had a larger deflection capacity (12.7 mm against 6.37 mm for the current experiment and Dey's specimens), although having an earlier fracture formation (0.83 mm).The CFRC-AAC panels were also 7 times more robust than the conventional AAC panels at peak stress. The ARGFRC-AAC panels absorbed 3–6 times more energy than the AAC blocks. The high tensile strength of the curauá fiber and the sufficient bonding between skin layers and core explained the performance variations between these identical panel structures with the same core material.

Frazao et al. [29] constructed a comparable sandwich panel construction with sisal fiber-cement composite outer layers and polypropylene fiber-reinforced lightweight concrete core layers. They had 4.73 MPa flexural strength and 18.14 kN maximum load with a mid-span deflection of 10.40mm. The PP-fiber reinforced core allowed for better strength than the CFRC-AAC, while the sisal fiber reinforcement (6 percent volume fraction) ensured multiple cracking behavior. In the four-point bending tests, the sisal reinforced laminates showed an ultimate flexural strength of 8.60 MPa, while the curauá reinforced composites showed 32.16 MPa. Pre-molded AAC has a reduced compressive strength and brittle failure, whereas the PP-fiber reinforced lightweight concrete showed a pseudo-hardening reaction when bent. Both natural fiber reinforced composites showed repeated cracking and ductility.

The three-layered composites showed deflection hardening and numerous crack development in the skin layers, indicating excellent energy absorption capability. Figure 4 shows the stress-deflection curves of cementitious materials under bending and their tensile response.The material's average flexural strength of 32.16 MPa and peak load toughness of 13.32 J are comparable to other cementitious composites in the literature: Silva et al. [37] obtained 29 MPa strength and 22 KJ/m2 toughness for 10% volume fraction sisal textile-reinforced composites. d'Almeida et al. [18] investigated curauá composites with five layers and 6% volume fraction, attaining 27.52 MPa and 29.13 kJ/m2. Souza et al. [39] investigated curauá specimens with three layers of long

fibers and found 28 MPa and 16.4 J. These values indicate ductility and good mechanical performance.

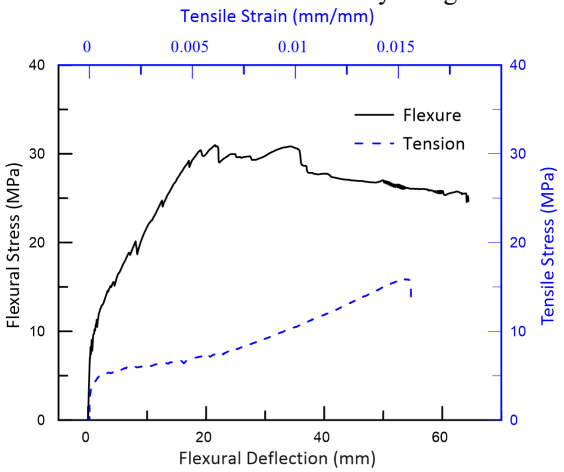

Figure 4: Flexural and tensile behavior of the cementitious composites (sandwich panels' skin layers)

The panels'mechanical properties were calculated with Allen's [42] equations and the standards ASTM D7249 [43] and ASTM D7250 [44]. The rigidity of a sandwich beam is given by D, represents the sum of the flexural rigidities of each constituent, skins and core, measured about the centroidal axis of the cross-section. If the ratio between the distance *d* between the centroids of both facings and the face thickness *t* is higher than 5.77 (d/t > 5.77), it can be rewritten as:

$$D' = E_f \frac{btd^2}{2} + E_c \frac{bc^3}{12} \quad (1)$$

Using ASTM D7250 [44], it is possible to calculate the sandwich panels' transverse shear rigidity.

$$U = \frac{P(S-L)}{4\left[\Delta - \frac{P(2S^2 - 3SL^2 + L^3}{96D}\right]} \quad (2)$$

Where U is the transverse shear rigidity, P is the total applied force, S is the support span length, L is the load span length, Δ is the beam mid-span deflection, and D is the flexural rigidity, previously calculated.

The shear rigidity was calculated for each tested panel for a series of forces (P), with their respective deflections (Δ), up to the point of the maximum applied load (P_{max}). These values have to be calculated for a minimum of 10 force levels evenly spaced along the force-deflection curve. An interval of 0.05 mm was established between each force applied in the formula up to the peak load. The average value of the panels' transverse shear rigidity U is 2.29 x 10^5 N

Table 1: Mechanical properties of the tested sandwich panels under monotonic bending tests

Sandwich Panel	Maximum bending load (N)	Deflection at Pmax (mm)	Toughness at 12 mm (J)	Flexural rigidity D (N.mm²)	Shear rigidity U (N)
1	4238	0.78	36.57	5.69E+10	2.26E+05
2	4055	0.89	38.65	5.84E+10	2.75E+05
3	3732	0.81	33.60	5.70E+10	1.86E+05
Average	4008	0.83	36.27	5.74E+10	2.29E+05
Deviation	256	0.060	2.54	8.22E+08	4.45E+04

2.5 Cyclic bending test

Figure 5 shows the force-deflection curve obtained by applying ten loading-unloading cycles to three sandwich panel specimens. The conventional fracture mechanics equations were not employed because the materials were evaluated without a notch. However, stiffness and energy evaluations were done on each specimen to determine the structure's deterioration parameters. Cyclic tests revealed similar characteristics to monotonic tests, with strong resistance capacity and, despite initial stiffness loss, higher maximum force. The hysteresis curves widened as the cycles went. Rouby and Reynaud [49] claim that degradation of the matrix-fiber interface contributes to eventual rupture, with broader cycles indicating a loss of strength.

Unloading leaves a residual displacement that precedes the loading of a fresh cycle. The material's ability to recover from damage caused by imposed cycles is linked to displacement. The degree of reversibility is computed as the ratio of the reversible displacement (r) to the total displacement (t) of the hysteresis cycle. Total displacement is determined as the distance in x to the cycle's unloading point [50]. The cycle stiffness affects the bending behavior of specimens under cyclic force. The Ecycle computation uses the slope between the two loading reversal points. The reversible displacement is the distance in x to Ecycle's opposite side. The initial tangential module E0 is used to construct the initial elastic section of the force-deflection curve [51].

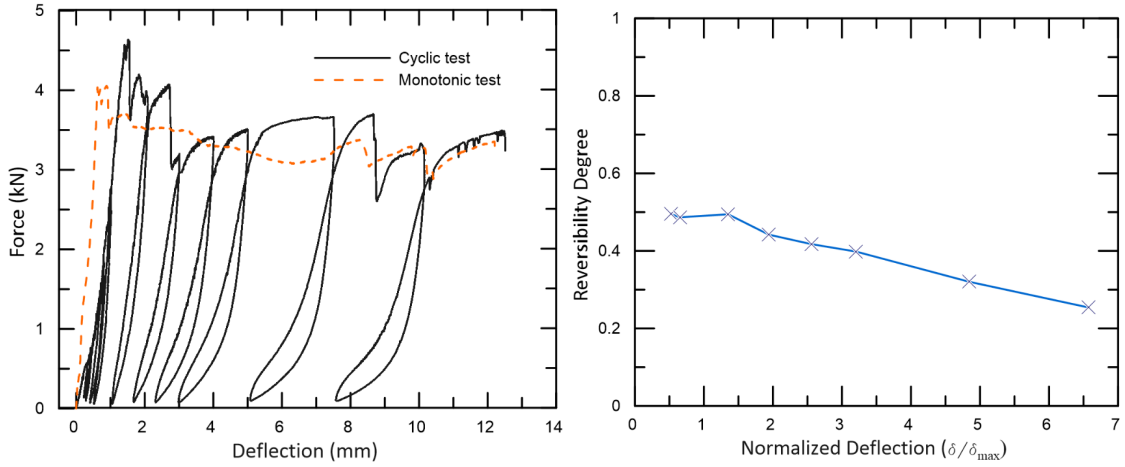

Figure 5: Cyclic bending tests: a) comparative force-deflection relationship between cyclic and monotonic four-point bending tests; b)) relationship between reversibility degree (δ_r/δ_t) and normalized deflection (δ/δ_{max})

As shown in Figure 5-a, the earliest cycles lose the most stiffness. As the load increases, cracks develop and expand, causing curve changes that are not fully recoverable due to their inelastic nature. Widening hysteresis cycles suggest significant energy loss [37, 38]. OriginPro software calculated the area covered by the cycles of each panel. With 1, 2, 3, 4, 5, 7.5, and 10 mm deflection points as references. To compare the toughness of the sandwich panels during monotonic and cyclic testing, the mean toughness at 12 mm was computed for the first case, which was 36.27 J. Compared to the cyclic equivalent, 6.29 J, the panels lose 17.34 percent toughness after 10 cycles of loading and unloading.

In comparison to the monotonic bending specimens, the AAC core showed more fracture propagation and damaged areas. However, compression caused less harm to the top skin layers. The linear-elastic behavior of sandwich panels with textile-reinforced concrete facings explains this behavior; the tensile layer accumulates the effects of repeated loading, leading to degradation of the matrix-fiber interface.

In addition, cyclic loads cause increased wear on the matrix-fiber contact [54]. In this approach, the composite's stress transmission mechanism eventually loses efficiency. The specimens examined through loading-unloading cycles, however, behaved satisfactorily, demonstrating no critical degradation until the fibers were pulled out.

3 Conclusions

The work showed experimental results of sandwich composites with an aerated autoclaved concrete core and natural curauá cement-based composites externally reinforced. The curauá unidirectional fibers were particularly successful at controlling the creation and widening of fractures, therefore improving the material's post-cracking strength and toughness. All laminar composites tested showed repeated cracking and deflection hardening. AAC's low compressive strength and brittle failure made it more ductile when supported by the sandwich composites.

The sandwich panels' flexural rigidity and energy absorption ratio were good. The specimens' load capacity was equivalent to or greater than sandwich panels of similar structure. The panels' steady dissipation of energy during four-point bending tests revealed good overall ductility.

The panels also had a composite reaction to loading and unloading, where the three main constituent materials acted as a single material with complementary qualities. The specimens often had hysteresis cycles that widened as the material decayed. Despite a lower toughness than the monotonic test, the sandwich panels' post-peak ductility was satisfactory, allowing energy to be released gradually throughout the deflection-softening trend. In both monotonic and cyclic testing, shear cracks in the core and transverse fractures in the composite layers, particularly in the bottom layers, were the prevalent failure modes. A excellent strength/weight ratio, high energy absorption, and a mechanical reaction suitable for use as a light and sustainable material in low-cost buildings were developed.

.

Authorship statement. The authors hereby confirm that they are the sole liable persons responsible for the authorship of this work, and that all material that has been herein included as part of the present paper is either the property (and authorship) of the authors, or has the permission of the owners to be included here.

References

[1] S. N. Monteiro, F. P. D. Lopes, A. P. Barbosa, A. B. Bevitori, I. L. Amaral Da Silva, and L. L. Da Costa, “Natural lignocellulosic fibers as engineering materials- An overview,” Metall. Mater. Trans. A Phys. Metall. Mater. Sci., vol. 42, no. 10, 2011, doi: 10.1007/s11661-011-0789-6.

[2] D. B. Dittenber and H. V. S. Gangarao, “Critical review of recent publications on use of natural composites in infrastructure,” Compos. Part A Appl. Sci. Manuf., vol. 43, no. 8, pp. 1419–1429, 2012, doi: 10.1016/j.compositesa.2011.11.019.

[3] S. V. Joshi, L. T. Drzal, A. K. Mohanty, and S. Arora, “Are natural fiber composites environmentally superior to glass fiber reinforced composites?,” 2004, doi: 10.1016/j.compositesa.2003.09.016.

[4] R. D. S. G. Campilho, Natural fiber composites. 2015.

[5] L. Yan, B. Kasal, and L. Huang, “A review of recent research on the use of cellulosic fibres, their fibre fabric reinforced cementitious, geo-polymer and polymer composites in civil engineering,” Compos. Part B Eng., 2016, doi: 10.1016/j.compositesb.2016.02.002.

[6] D. HULL and T. W. CLYNE, An introduction to composite materials. Cambridge university press, 1996.

[7] B. MOBASHER, Mechanics of fiber and textile reinforced cement composites. Boca Raton: CRC Press, 2011.

[8] J. C. Caraschi and A. L. Leão, “Characterization of curaua fiber,” Mol. Cryst. Liq. Cryst. Sci. Technol. Sect. A Mol. Cryst. Liq. Cryst., vol. 353, no. 1, pp. 149–152, 2000, doi: 10.1080/10587250008025655.

[9] K. G. Satyanarayana, J. L. Guimarães, and F. Wypych, “Studies on lignocellulosic fibers of Brazil. Part I: Source, production, morphology, properties and applications,” Compos. Part A Appl. Sci. Manuf., vol. 38, no. 7, 2007, doi: 10.1016/j.compositesa.2007.02.006.

[10] R. Zah, R. Hischier, A. L. Leão, and I. Braun, “Curauá fibers in the automobile industry - a sustainability assessment,” J. Clean. Prod., vol. 15, no. 11–12, pp. 1032–1040, 2007, doi: 10.1016/j.jclepro.2006.05.036.

[11] M. de S. Picanço, “Compósitos cimentícios reforçados com fibras de curauá,” Pontifícia Universidade Católica do Rio de Janeiro, Rio de Janeiro, 2005.

[12] D. G. Soltan, P. das Neves, A. Olvera, H. Savastano Junior, and V. C. Li, “Introducing a curauá fiber reinforced cement-based composite with strain-hardening behavior,” Ind. Crops Prod., 2017, doi: 10.1016/j.indcrop.2017.03.016.

[13] B. Zukowski, F. de Andrade Silva, and R. D. Toledo Filho, “Design of strain hardening cement-based composites with alkali treated natural curauá fiber,” Cem. Concr. Compos., 2018, doi: 10.1016/j.cemconcomp.2018.03.006.

[14] H. Savastano and V. Agopyan, “Transition zone studies of vegetable fibre-cement paste composites,” Cem. Concr. Compos., vol. 21, no. 1, pp. 49–57, 1999, doi: 10.1016/S0958-9465(98)00038-9.

[15] R. D. Tolêdo Filho, K. Scrivener, G. L. England, and K. Ghavami, “Durability of alkali-sensitive sisal and coconut fibres in cement mortar composites,” Cem. Concr. Compos., 2000, doi: 10.1016/S0958-9465(99)00039-6.

[16] M. F. Canovas, N. H. Selva, and G. M. Kawiche, “New economical solutions for improvement of durability of Portland cement mortars reinforced with sisal fibres,” Mater. Struct., 1992, doi: 10.1007/BF02472258.

[17] W. de N. D. R. Martel, I. P. Salgado, and F. A. Silva, “The Influence of Fiber Treatment on the Morphology, Water Absorption Capacity and Mechanical Behavior of Curauá Fibers,” Journal of Natural Fibers. 2020, doi: 10.1080/15440478.2020.1758863.

[18] A. L. F. S. D'Almeida, J. A. Melo Filho, and R. D. Toledo Filho, "Use of curaua fibers as reinforcement in cement composites," 2009, doi: 10.3303/CET0917287.
[19] A. d'Almeida, R. Toledo Filho, and J. Melo Filho, "Cement composites reinforced by short curaua fibers," Rev. Mater., vol. 15, no. 2, pp. 153–159, 2010, doi: 10.1590/S1517-70762010000200010.
[20] E. Gartner, "Industrially interesting approaches to 'low-CO2' cements," Cem. Concr. Res., vol. 34, no. 9, pp. 1489–1498, 2004, doi: 10.1016/j.cemconres.2004.01.021.
[21] N. M. Altwair and S. Kabir, "Green concrete structures by replacing cement with pozzolanic materials to reduce greenhouse gas emissions for sustainable environment," 6th Int. Eng. Constr. Conf. (IECC'6), Cairo, Egypt, June, 2010.
[22] RILEM Recommended Practice, Autoclaved Aerated Concrete: Properties, Testing and Design. London, UK: E & FN SPON, 1993.
[23] M. . Haas, "The future of AAC–from a material scientist's point of view," in Autoclaved Aerated Concrete - Limbachiya and Roberts (eds), Limbachiya and Roberts, Ed. London: Taylor & Francis Group, 2005.
[24] Z. Liu, K. Zhao, C. Hu, and Y. Tang, "Effect of Water-Cement Ratio on Pore Structure and Strength of Foam Concrete," Adv. Mater. Sci. Eng., vol. 2016, 2016, doi: 10.1155/2016/9520294.
[25] S. O. Rathi and P. V. Khandve, "AAC Block-A New Eco-friendly Material for Construction," Int. J. Adv. Eng. Res. Dev., vol. 2, no. 4, pp. 410–414, 2015.
[26] C. A. Fudge and J. N. Hacker, "UK housing and climate change: Performance evaluation using AAC," in Autoclaved Aerated Concrete - Limbachiya and Roberts (eds), London: Taylor & Francis Group, 2005.
[27] F. H. Wittmann, Autoclaved Aerated Concrete, Moisture and Properties, 6th ed. Amsterdam: Elsevier Scientific Publishing Company, 1983.
[28] J. Arbaoui, Y. Schmitt, J. Pierrot, and F. Royer, "Comparison Study and Mechanical Characterisation of a Several Composite Sandwich Structures," Int. J. Compos. Mater., vol. 5, no. 1, pp. 1–8, 2015, doi: 10.5923/j.cmaterials.20150501.01.
[29] C. Frazão, J. Barros, R. Toledo Filho, S. Ferreira, and D. Gonçalves, "Development of sandwich panels combining Sisal Fiber-Cement Composites and Fiber-Reinforced Lightweight Concrete," Cem. Concr. Compos., vol. 86, pp. 206–223, 2018, doi: 10.1016/j.cemconcomp.2017.11.008.
[30] ASTM C230/230M, "Standard Specification for Flow Table for Use in Tests of Hydraulic Cement," ASTM Int., 2014.
[31] I. P. Salgado and F. A. Silva, "Avaliação do Comportamento Mecânico de Painéis Sanduíche com Compósitos Laminados Reforçados com Fibra de Curauá e Núcleo de Concreto Celular Autoclavado," Pontifícia Universidade Católica do Rio de Janeiro, 2019.
[32] RILEM, Autoclaved Aerated Concrete: Properties, Testing and Design. E&FN Spon, 1993.
[33] AMERICAN SOCIETY FOR TESTING AND MATERIALS, "ASTM C1341-13 - Standard Test Method for Flexural Properties of Continuous Fiber-Reinforced Advanced Ceramic Composites," ASTM Int., vol. i, pp. 1–21, 2013, doi: 10.1520/C1341-13.2.
[34] Associação Brasileira de Normas Técnicas, "NBR 13528: Revestimento de paredes de argamassas inorgânicas - Determinação da resistência de aderência à tração." p. 15, 2010.
[35] V. Dey, G. Zani, M. Colombo, M. Di Prisco, and B. Mobasher, "Flexural impact response of textile-reinforced aerated concrete sandwich panels," Mater. Des., vol. 86, pp. 187–197, 2015, doi: 10.1016/j.matdes.2015.07.004.
[36] B. Mobasher, J. Pahilajani, and A. Peled, "Analytical simulation of tensile response of fabric reinforced cement based composites," Cem. Concr. Compos., 2006, doi: 10.1016/j.cemconcomp.2005.06.007.
[37] F. de A. Silva, B. Mobasher, and R. D. T. Filho, "Cracking mechanisms in durable sisal fiber reinforced cement composites," Cem. Concr. Compos., vol. 31, no. 10, pp. 721–730, 2009, doi: 10.1016/j.cemconcomp.2009.07.004.
[38] Y. Yao, F. A. Silva, M. Butler, V. Mechtcherine, and B. Mobasher, "Tension stiffening in textile-reinforced concrete under high speed tensile loads," Cem. Concr. Compos., 2015, doi: 10.1016/j.cemconcomp.2015.07.009.
[39] L. O. Souza, L. M. S. Souza, and F. A. Silva, "Mechanics and cracking mechanisms in natural curauá textile reinforced concrete," RILEM Bookseries, 2018, doi: 10.1007/978-94-024-1194-2_42.
[40] I. M. Daniel and J. L. Abot, "Fabrication, testing and analysis of composite sandwich beams," Compos. Sci. Technol., 2000, doi: 10.1016/S0266-3538(00)00039-7.
[41] D. ZENKERT, An Introduction to Sandwich Construction. Engineering Materials Advisory Services Ltd., 1995.
[42] H. D. Allen, Analysis and Design of Structural Sandwich Panels. Pergamon Press, 1969.
[43] American Society for the Testing of Materials, "ASTM D7249: Standard Test Method for Facing Properties of Sandwich Constructions by Long," Annu. B. ASTM Stand., vol. i, pp. 1–9, 2006, doi: 10.1520/D7249.
[44] American Society for the Testing of Materials, "ASTM D7250: Standard Practice for Determining Sandwich Beam Flexural and Shear Stiffness," ASTM Stand., vol. i, pp. 1–8, 2009, doi: 10.1520/D7250.
[45] G. M. Folie, "The behaviour and analysis of orthotropic sandwich plates," Build. Sci., 1971, doi: 10.1016/0007-3628(71)90004-1.
[46] PRECON INDUSTRIAL S/A, "Bloco Precon - Concreto Celular Autoclavado," 2017. https://precon.com.br/portal/wp-content/uploads/2017/09/bloco-cca.pdf.
[47] N. Uddin, F. Fouad, U. K. Vaidya, A. Khotpal, and J. C. Serrano-Perez, "Structural characterization of hybrid Fiber reinforced Polymer (FRP)-Autoclave Aerated Concrete (AAC) panels," J. Reinf. Plast. Compos., vol. 25, no. 9, pp. 981–999, 2006, doi: 10.1177/0731684406065090.
[48] I. G. Colombo, M. Colombo, and M. Di Prisco, "Bending behaviour of Textile Reinforced Concrete sandwich beams," Constr. Build. Mater., 2015, doi: 10.1016/j.conbuildmat.2015.07.169.
[49] D. Rouby and P. Reynaud, "Fatigue behaviour related to interface modification during load cycling in ceramic-matrix fibre composites," Compos. Sci. Technol., 1993, doi: 10.1016/0266-3538(93)90126-2.
[50] B. Boulekbache, M. Hamrat, M. Chemrouk, and S. Amziane, "Comportement en flexion des bétons fibrés sous chargement cyclique," MATEC Web Conf., 2014, doi: 10.1051/matecconf/20141101035.
[51] B. Boulekbache, M. Hamrat, M. Chemrouk, and S. Amziane, "Flexural behaviour of steel fibre-reinforced concrete under cyclic loading," Constr. Build. Mater., 2016, doi: 10.1016/j.conbuildmat.2016.09.035.

[52] J. Dutkiewicz, “Superelasticity and shape memory effect in copper base alloys,” Acta Phys. Pol. A, 1999, doi: 10.12693/APhysPolA.96.197.
[53] H. CUYPERS, “Analysis and design of sandwich panels with brittle matrix composite faces for building applications,” Brussels, 2002.
[54] J. Hegger, A. BENTUR, M. . Curbach, B. . Mobasher, A. . Peled, and J. . Wastiels, “Mechanical behaviour of textile reinforced concrete,” in State-of-the-Art Report of RILEM Technical Committee 201-TRC: Textile Reinforced Concrete, 2006, pp. 133–186.
[55] J. M. Davies, Lightweight Sandwich Construction. 2008.


CILAMCE
PANACM
RIO DE JANEIRO 2021